PNAS
www.pnas.org

Supplementary Information for

Adaptational lag to temperature in valley oak (*Quercus lobata*) can be mitigated by genome-informed assisted gene flow

Luke Browne, Jessica W. Wright, Sorel Fitz-Gibbon, Paul F. Gugger, Victoria L. Sork*

Corresponding author: Victoria L. Sork
Email: vlsork@ucla.edu

This PDF file includes:

www.pnas.org/cgi/doi/10.1073/pnas.1908771116

Supplementary Information Text

Materials and Methods

Description of valley oak provenance trial

Valley oak (*Quercus lobata Neé*), along with other oak species, are culturally, economically, and ecologically important trees in California—both to the native peoples of California for more than 10,000 years (1) and to present-day human populations (2, 3). After acorns were collected from valley oak maternal trees in 2012, they were germinated in a greenhouse at the USDA Forest Service, Pacific Southwest Research Station, Institute of Forest Genetics (IFG) in Placerville, CA (Figure S1). Following germination, seedlings were placed into lathe houses at IFG and the USDA Forest Service, Chico Seed Orchard (CSO), in Chico, CA (Figure S1). When planted into the field in late 2014 / early 2015, seedlings were spaced evenly at 2.25 m intervals, and blocks were irrigated, and weeds were controlled to maximize the probability of seedling establishment as is commonly done in provenance trials. Seedlings were planted into a randomized block design within each site such that each family (*i.e.*, seedlings collected as acorns from a single adult) had at least one representative in each block at each site. Full details on the establishment and planting design of the provenance trial are available in Delfino-Mix, Wright, Gugger, Liang and Sork (4).

Climate data

We used climate data from the Basin Characterization Model dataset developed for California (5), which integrates climate data with landscape attributes like topography to generate monthly climate data at a 270 x 270 m resolution. For evaluating the potential effects of climate change on valley oak growth, we focused on T_{max}, the average maximum temperature of the hottest months from June-August, which is a climate variable shown to be important in shaping genetic variation and geographic distribution in valley oak (6-10). T_{max} in our dataset is strongly correlated with other temperature-related variables, such as mean annual temperature, mean annual maximum temperature, temperature seasonality, and growing degree days > 5° C (Pearson's $R > 0.60$ for all). We did not focus on associating precipitation variables with progeny growth in the provenance trials because the common garden sites were irrigated during establishment, which would obscure differences in precipitation between the climate of origin and common garden sites. We did, however, use precipitation variables when considering how climate of origin was associated with growth in the common gardens and how climate of origin was associated with patterns of genetic variation (see below).

To characterize climate of origin, we performed a principal component analysis (PCA) based on a set of 10 climate variables, where the first two axes explained 41.1% and 23.3% of the variance respectively (Fig. S6). The climate variables we used to characterize climate of origin were maximum summer temperature ($T_{\max}$), average maximum temperature across all months (T_{max_annual}), minimum winter temperature ($T_{\min}$), average minimum temperature across all months (T_{min_annual}), average temperature across all months (T_{ave}), temperature seasonality (Bioclim 4), precipitation seasonality (Bioclim 15), summer precipitation (Bioclim 18), precipitation of the coldest quarter (Bioclim 19), and climatic water deficit (CWD), which have all been shown to be important in predicting genetic variation in valley oak (10, 11). We calculated bioclimatic variables from monthly Basin Characterization Model climate data in the 'climates' R package (12). For estimating how temperature has changed since the Last Glacial Maximum 21,000 years ago, we used paleoclimate data from the ClimateWNA v5.00 dataset (13).

To model the effect of future climate on valley oak growth, we focused on the representative concentration pathway RCP 8.5 from the IPCC 5th assessment report for 2070-2099, which represents a business-as-usual scenario where emissions continue to rise throughout the 21st century reaching > 1,370 ppm CO_2 equivalent by 2100 (14). We used a total of 5 RCP 8.5 projections (MIROC-RCP85, CCSM4-RCP85, IPSL-RCP85, CNRM-RCP85, FGOALS-RCP85) from the Basin Characterization Model climate dataset and made predictions separately for each climate projection and then averaged across the results.

Modeling growth based on T_{max} difference

We used height of the tallest stem as our metric of growth because it likely plays an important role in the fitness and survival of valley oak seedlings, where taller seedlings are more likely to escape grazing by native and domestic herbivores, which is a prominent limitation on recruitment for valley oak (15). Additionally, height of the tallest stem is an easily collectible, non-destructive metric of growth that was available for all census years. Height of the tallest stem in valley oak is strongly correlated with other metrics of growth, such as stem diameter (16). We excluded seedlings that had died, that had obvious signs of mechanical or gopher damage (*e.g.*, effects on growth obviously not related to climate), that were missing height data in either the 2014 or 2017 census, or that had negative growth rates (possibly due to measurement error). These exclusions resulted in a final dataset of 5,051 seedlings.

In our growth model, we included the height of the tallest stem in the 2014 census to control for differences in growth prior to planting and because relative growth rate usually declines with plant size (17). To control for the effects of differences in climate of origin (*e.g.*, plants originating in warm, wet areas growing faster than plants from cool, dry areas) and potential interactions of climate of origin with T_{max} difference on progeny growth, we included in the model the first two principal components of the climate of origin (see above) and the interaction effect of the principal components of climate with T_{max} difference. To control for unmeasured genetic and environmental correlations among progeny from the same family or the same population, we included Family ID and locality where the individuals were collected as random effects. The overall model associating relative growth rates to T_{max} difference and other covariates took the following form:

$$\begin{aligned} \mathrm{RGR} = \alpha + f_1(T_{max}\ difference) + f_2\left(PC1_{Climate\_of\_origin}\right) + f_3\left(PC2_{Climate\_of\_origin}\right) \\ + f_4\left(T_{max}\ difference * PC1_{Climate\_of\_origin}\right) \\ + f_5\left(T_{max}\ difference * PC2_{Climate\_of\_origin}\right) \\ + f_6(Height_{2014}) + f_7(Family) + f_8(Locality) + Block + \varepsilon \end{aligned}$$

where RGR is the relative growth rate, α is the estimated intercept, $f_1, \ldots, f_8$ are smooth functions estimated by the model with restricted maximum likelihood, and ε is the model error term. Variable descriptions are given in main text. We used a Tweedie error distribution (18, 19), which allows a flexible mean-variance relationship and improved model fit compared to a Gaussian error distribution (Fig. S7). Continuous covariates were mean centered and scaled to SD = 1 prior to analysis to aid in model convergence and prediction (20). We fit the model to the data using the 'mgcv' package (21) in R 3.4.1 (22).

Genotyping by sequencing

Leaf samples from valley oak adults were collected throughout the species range (Fig. S1), and were stored on ice until arriving at UCLA, where they were transferred to a -80° C freezer for

storage. We extracted total genomic DNA from 50 mg of frozen tissue using the Qiagen DNeasy Plant Mini Kit, adding an additional prewash step to remove secondary compounds from the finished product. The prewash step consisted of adding 1 mL of prewash buffer after grinding samples, shaking the resulting mixture for 10-20 s at 30 Hz, and then spinning 10 min at 10,000 rpm in a microcentrifuge. Following this step, we discarded the supernatant and processed the pellet following the standard DNeasy protocol starting at the Buffer AP1/RNase A addition step. The prewash buffer was made of 0.01 g/mL polyvinylpyrrolidone (PVP) (k-30, SABC), 50 mM EDTA, 100 mM Tris-HCl (from pH 8.0 stock), 1 M NaCl, and 4.5 µL/mL 2-mercaptoethanol (added immediately prior to use).

Next, we digested the total genomic DNA with a restriction enzyme, following the genotyping by sequencing protocol of Elshire*, et al.* (23), with a few modifications. In contrast to the original protocol, we pooled 48 samples per library prep and sequencing lane rather than 96. Additionally, we added adapters during the ligation step rather than prior to restriction digestion, and we added AMPure XP bead-based size selection/purification steps after the ligation step and repeated after the PCR step. Finally, we altered the number PCR cycles to 16 from 18. We sent the final libraries for sequencing to the UCLA Broad Stem Cell Research Center on an Illumina HiSeq2000 v3 using single-end, 100-bp sequencing.

We used STACKS 1.28 to 1.41 (24) to demultiplex and filter reads, removing adapter sequences with up to two mismatches (*adapter_mm*), recovering barcodes with up to one mismatch to the expected barcodes (*r*), removing reads with an uncalled base (*c*), and discarding low quality reads with default settings (*q*). Additionally, we trimmed reads to 92 bp (*t*). We aligned reads to v3.0 of the *Quercus lobata* reference genome available at http://valleyoak.ucla.edu using BWA 0.7.12 (25). We called SNPs with a minimum Phred-scaled confidence threshold of 30 using GATK 3.7 (26).We also filtered low quality variations that were: QD < 10.0 (quality by depth), DP < 4 (genotype read depth), and ExcessHet > 100. We then applied an iterative filtering process (27) to filter out individuals with ≥ 25% missing data, and filter to biallelic SNPs with ≤ 5% missing data, minor allele frequency ≥ 5%, a mean depth of coverage ≥ 5, and a quality score > 20 using VCFtools v0.1.15 (28). We filtered SNPs in linkage disequilibrium using plink v1.90 (29), pruning pairs of SNPs within a 500 bp sliding window that had an $R^2 > 0.70$ with another variant until no such pair remains, advancing the window 50 bp at a time.

Genome-wide association analysis with T_{max} difference

For stage one of our two-stage residual-outcome GWAS (30), we included the main effects of T_{max} difference, along with Family ID, Block, Locality, Height in 2014, the first two principal components of the climate of origin as described above, and the interaction effect of the principal components of climate with T_{max} difference. Additionally, to control for population structure that may produce spurious associations in GWAS (31, 32), we estimated the kinship matrix among individuals using all SNPs that passed filtering using the 'A.mat' function in the R package 'rrBLUP' (33). We then ran a principal components analysis using the 'prcomp' function in R and used the first two PC axes in the model, which explained 3.4% and 2.1% of the variation, respectively (Fig. S8). We included these first two PC axes and their interactions with T_{max} difference in the model, which took the following form:

$$\text{RGR} = \alpha + f_1(T_{max}\ difference) + f_2\left(PC1_{Climate\_of\_origin}\right) + f_3\left(PC2_{Climate\_of\_origin}\right) + f_4\left(T_{max}\ difference * PC1_{Climate\_of\_origin}\right) + f_5\left(T_{max}\ difference * PC2_{Climate\_of\_origin}\right) + f_6(Height_{2014}) + f_7(Family) + Block + f_8(Locality) + f_9\left(PC1_{Kinship}\right) + f_{10}\left(PC2_{Kinship}\right) + f_{11}\left(T_{max}\ difference * PC1_{Kinship}\right) + f_{12}\left(T_{max}\ difference * PC2_{Kinship}\right) + \varepsilon$$

where RGR is the relative growth rate, α is the estimated intercept, $f_1, \ldots, f_{12}$ are smooth functions estimated by the model with restricted maximum likelihood and a Tweedie error distribution (18, 19). Variables were mean centered and scaled to SD = 1 prior to analysis. We fit the model to the data using the 'mgcv' package (21) in R 3.4.1 (22).

In stage two, we used the residuals of the above model (representing adjusted relative growth rates) as the dependent variable and estimated the main effect of each genotype and interaction of T_{max} difference and genotype (*e.g.*, 0, 1, 2 copies of non-reference alleles in the maternal genotype) for each SNP. The main effects of T_{max} difference, in addition to Family ID, Block, Locality, Height in 2014, the first two principal components of the climate of origin were not included in the stage two model because they were previously included in the stage one model. Here, it useful to consider the interaction between adjusted relative growth rates and T_{max} differences for each genotype as a 'function-valued' trait (34, 35) (*i.e.*, a trait that varies as a function of another continuous variable). We centered and scaled genotypes (*i.e.*, mean = 0, SD = 1) prior to analysis and imputed missing data with the average genotype value. We again used a GAM framework to estimate genotype interactions separately for each SNP (n = 12,357 models), estimating effects with restricted maximum likelihood and a Gaussian error distribution because values for adjusted relative growth rates were approximately normally distributed. The models took the following form:

$$Adjusted\ RGR = \alpha + Genotype + f_1(T_{max}\ difference * Genotype) + \varepsilon$$

It is important to note that we associated maternal genotypes with the relative growth rates of their progeny in the provenance trial, which comes with some limitations that likely reduce the power to detect such associations. In the case of homozygous maternal genotypes, the progeny will contain at least one allele from the maternal genotype, with the identity of the other allele contributed by the pollen donor remaining unknown. In the case of heterozygous maternal genotypes, the alleles will segregate amongst their progeny at an approximate ratio of 50:50. We included heterozygous maternal genotypes in the analysis to not limit the sample sizes in our GWAS.

Genomic-estimated breeding values (GEBVs)

Genomic-estimated breeding values are commonly used in plant and animal breeding programs to facilitate genomic improvement across generations (36-39). GEBVs use genomic sequencing data to estimate the summed effects of alleles across many loci for a desired trait. This approach has increasingly been used for forest trees (40) and human genetics (also referred to as polygenic scores) to model the genomic basis of complex, polygenic traits. Generally, the breeding value approach focuses on the combined effects of many loci across the genome on phenotypic variation, rather than isolating the effects of individual loci, which complements our sequencing approach (GBS) that sequences only a random fraction of the genome, which would likely limit

our ability to isolate and identify any one SNP casually linked with phenotypic variation, but provides us power to assess how genome-wide genetic variation is associated with phenotypic variation.

We calculated GEBVs based on the maternal genotype of each seedling, and as a result, we interpret the GEBVs to indicate the genetic value of each maternal tree in relation to their average progeny performance when progeny are planted into warmer temperatures that their site of origin. To estimate GEBVs, we summed the predicted adjusted progeny relative growth rates in warmer temperatures (T_{max} difference > 0° C) for each maternal genotype:

$$GEBV_i = \sum_j Growth\ response_{ij}$$

where GEBV is the genomic-estimated breeding value for maternal tree *i*, and *Growth response* is the predicted relative growth rate of progeny averaged across values of T_{max} difference > 0° C & < 9.3 °C after adjusting for covariates (*e.g.*, block effects, initial height, locality, family ID, genetic kinship, and climate of origin) for the genotype of maternal tree *i* at SNP *j*. We used 9.3°C T_{max} difference as the upper limit for predictions because that was the maximum observed difference across the two planting sites in the common garden experiment. We mean centered and scaled GEBVs to SD = 1 after estimation to aid in interpretation. We varied the number of SNPs used in GEBV estimation from 25, 50, 100, 200, 300, …, 1000, 2000, 3000, …, to 12357 SNPs and chose the final number of SNPs to use in estimated GEBVs based on the SNP set that maximized the variance explained in the adjusted relative growth rates in either the full data set or an independent testing set (see below for cross-validation approach). SNPs were ordered before selection based on the strength of their genotype-by-temperature interaction, such that the top SNPs were the SNPs with the lowest P values of the interaction term of genotype and T_{max} difference in the testing set from the GAM output following Lasky *et al.* (41).

Figure S9 shows a Manhattan plot, a histogram, and a QQ plot of the resulting uncorrected P values used when ordering SNPs for the GEBV estimation. Given that the goal of the study was not to identify any particular SNP or gene associated with growth rates, which would necessitate strict statistical significance thresholds to avoid false positives, we present results using P-values uncorrected for multiple testing. Additionally, using P-values adjusted for multiple testing produced very similar results as using uncorrected P-values, and P-values from our data simulation results (see below) show a similar distribution as our empirical results. Given that the magnitude of P-value estimates and whether they pass significance thresholds were not an important factor in improving breeding value estimates, we do not consider using either uncorrected or corrected P-values to have a major effect on the results or interpretation.

We assessed the explanatory and predictive power of the GEBVs with respect to adjusted relative growth rates. To assess the explanatory power (*i.e.*, the ability of GEBVs to explain variation in adjusted relative growth rates in the same dataset the GEBVs were estimated from), we calculated the R^2_{adj} of a GAM with adjusted relative growth rates as the response variable, and GEBVs and the interaction between GEBVs and T_{max} difference as explanatory variables using the full dataset of n = 2,295 seedlings with maternal genotypes. Importantly, here, the same data is being used to both fit the model and assess its explanatory power, which does not provide information on the ability of GEBVs to predict adjusted relative growth rates in an independent dataset, but does provide us information on how well the GEBVs explain variation in adjusted relative growth rates for our sampled population.

We assessed the predictive power (*i.e.*, the ability of GEBVs to explain variation in adjusted relative growth rates in observations not used to fit the model) of the GEBVs using 10-fold cross-validation (37, 42), which is a common approach to evaluate GEBVs by training a model on one portion of the dataset and validating the resulting model on a withheld 'testing' dataset. We employed a 10-fold cross-validation approach where the training sets consisted of approximately 90% of the full dataset and the testing sets consisted of the remaining 10%. Because having individuals from the same family in both the training and testing set could influence the predictive power of GEBVs (42), we used two approaches and present results from both. In the first approach, the training and the testing sets were chosen such that no individuals from the same family group (*i.e.,* collected from the same maternal tree) were in both the training and testing set. In the second approach, individuals from the same family group were allowed to occur in both training and testing sets. For both approaches, we calculated GEBVs in the training set and calculated the R^2_{adj} in the testing set, as described above. The number of SNPs used to estimate GEBVs varied across each validation fold depending on the number of SNPs that maximized R^2_{adj} in the testing set in each validation fold. The predictive power of GEBVs was not strongly different between approaches that either included or excluded individuals from the same family in the testing and training sets (Table S2). We assessed whether the predictive power estimated by cross-validation was higher than what would be expected under a null model of no association between GEBVs and growth rates using a permutation-based approach, where for each cross-validation fold, we permuted the response variable (adjusted relative growth rates) 100 times and calculated the average R^2_{adj} across these permutations.

Based on the full dataset of 5,051 individuals and the estimated variance across family lines, we calculated narrow-sense heritability of relative growth rates to be $h^2 = 0.19$ after controlling for block effects and initial height following Falconer and Mackay (43) and assuming half-sib relationships within families, which is very common for valley oak (44). This estimate of h^2 represents the upper limit on the explanatory power of GEBVs for relative growth rates for this study population.

Estimating GEBVs with BLUPs

An alternative approach to estimating GEBVs is the gBLUP (genomic Best Linear Unbiased Predictor) method, which predicts breeding values based on the genomic relatedness matrix among individuals (36, 37). First, to estimate our trait of interest – the growth response of progeny when planted into warmer temperatures than where they originated – we fit a linear mixed effect model where growth responses of progeny across T_{max} differences was fit as a quadratic function, such that progeny relative growth rates were a function of T_{max} difference and its squared term. The 1st order polynomial term was treated as a random effect that varied across maternal trees, which allows the overall position of the progeny growth response curve to vary for each maternal tree. We did not treat the 2nd order polynomial term as a random term due to issues with model convergence and fit. We also included as fixed effects: initial height, initial height squared, block effects, the first two PCs of the kinship matrix, and the first 2 PCs of the climate of origin. We fit the model using the lme4' (45) package in R v3.5.1 (22). From this model, we calculated the relative growth rate of progeny when planted into warmer temperatures for each maternal-tree from the predicted growth response functions and used this maternal tree-level metric as the phenotype for the gBLUP analysis. We used the 'BGLR' (46) package to conduct the gBLUP analysis. This analysis used the average predicted growth response of progeny planted into warmer temperatures for each maternal tree as the response variable and the genomic relatedness matrix among maternal trees as the response variable, fit using a Reproducing Kernel Hilbert Spaces (RKHS) model as described in the BGLR manual (https://cran.r-project.org/web/packages/BGLR/vignettes/BGLR-extdoc.pdf). The gBLUP analysis produced very similar breeding value estimates (Pearson's $R = 0.82$, $P < 0.001$, Fig. S10a) and growth

response estimates (Fig. S10b) as the GAM approach described above. Through data simulations (see section directly below), we found that the GAM approach was more effective as estimating breeding values than the gBLUP approach for the goals of our study, and therefore only present the GAM results in the main text.

Validating analysis approach with data simulations

Overview

To validate our approach to estimating GEBVs based on estimating generalized additive models (GAMs) on a SNP-by-SNP basis, we performed a series of data simulations with a sampling design similar to the one presented in this study. For a simulated set of maternal trees, we simulated known breeding values for the growth response of progeny when planted into warmer temperatures than their climate of origin. We then tested how the estimated GEBVs generated from our analysis approach were correlated with the simulated 'true' breeding values. We also assessed how varying the genetic architecture of progeny growth response to warmer temperatures and varying sampling designs would influence the efficacy of alternative analysis approaches (*e.g.*, approach used in this study based on modeling SNPs independent with GAMs vs. a gBLUP [genomic best linear unbiased predictor] approach).

Data generation

Our general approach was to simulate datasets with similar designs as the empirical data collected in this study. For initial simulations, we simulated 300 maternal trees with progeny planted into 2 planting sites (though we vary this in later simulations), with 5 blocks per planting site and one progeny per maternal tree planted in each block at each site, for a total sample size of 3,000 seedlings. Then, we simulated the relative growth rates of progeny across T_{max} differences, with variation in this growth response mediated by genetic variation of the maternal tree (described below). The effect sizes of block effects, site effects, and overall family effects on the progeny's relative growth rates were randomly drawn from a normal distribution with a mean of 0 and standard deviation of 0.25, which produced similar effect sizes as those observed in our empirical data. The T_{max} of simulated planting sites ranged from 25°C to 35°C and the T_{max} of origin for each maternal tree (and its progeny) was generated from a normal distribution with a mean of 30° and a standard deviation of four. These values were chosen to generate an adequate distribution of T_{max} differences for progeny in the simulated planting sites:

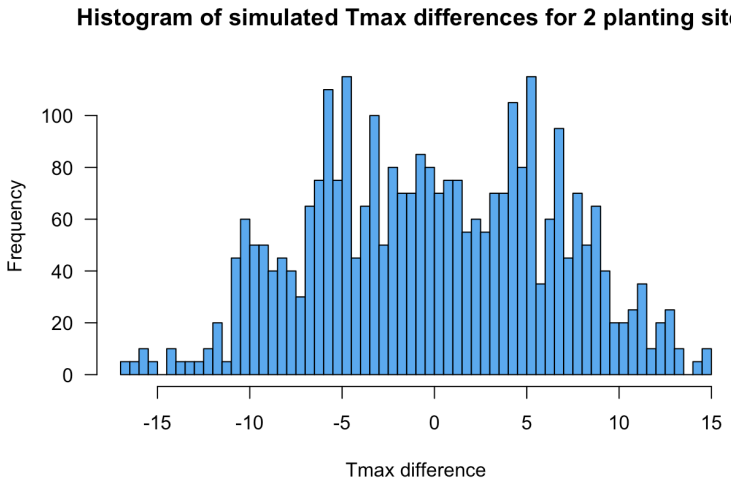

We simulated variation across maternal trees in terms of the growth response of their progeny to T_{max} differences, where some maternal trees would have progeny that grow relatively well when planted into warmer sites (values of T_{max} difference > 0°), while other maternal trees would have progeny that would grow better when planted into cooler sites (T_{max} difference < 0°). We modeled variation in progeny growth response to T_{max} differences at the maternal tree level as a quantitative trait, with the underlying genetic architecture generating this trait varying across simulations. We used 12,000 simulated unlinked SNPs with a minor allele frequency > 0.05 to generate the quantitative trait. We simulated scenarios where progeny growth response to T_{max} differences was modeled as: (1) a polygenic trait where most SNPs contributed small effects to explain 99% of the variance in progeny growth response across maternal trees, and (2) a trait determined by major QTLs, where 100 out of the 12,000 simulated SNPs explained 99% of the variance in differences in progeny growth response across maternal trees and the remaining 11,900 SNPs had no direct effect on the trait. We conservatively scaled the effect size of T_{max} differences on progeny growth response such that it was comparable or lower than the effect sizes of block, site, family, and residual error.

We generated the form of the progeny growth responses to T_{max} differences for each maternal tree from a normal distribution with a standard deviation of four. The mean of the progeny growth response functions represented the value of T_{max} difference that progeny growth was maximized, with values of T_{max} difference closer to 0° indicating maternal trees that display patterns expected under local adaptation. The figure below shows an illustrative distribution of progeny growth response to T_{max} differences across 300 simulated maternal trees represented by different colors, with the species-level average growth response in black, slight offset from an optimum of T_{max} difference = 0° to mimic the species-level pattern observed in the empirical data.

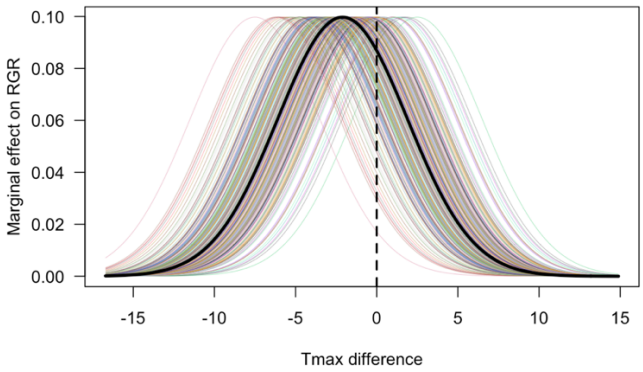

Our trait of interest for both the empirical and simulated data analyses was the growth response of progeny planted in warmer temperatures (values of T_{max} difference > 0°), which acts as a function-valued trait (34, 35) (*e.g.*, a trait that varies as a function of another continuous variable). We summarized this trait by averaging the predicted effects on relative growth rates for values of T_{max} difference > 0°. The figure below illustrates how this value was calculated across two representative simulated maternal trees. Each color represents a different maternal tree, with the red line showing a maternal tree with relatively higher progeny growth rates in warmer temperatures compared to the blue maternal tree. The bold sections of each line indicate the values that are being averaged over (progeny growth response at T_{max} difference > 0°) to summarize progeny growth response. Because this variation in the position of the growth response curve is a quantitative trait explained by the underlying genomic variation, we use this summary value of progeny growth response when planted into warmer sites as our 'true' breeding value (BV). The main goal of the statistical analysis is to estimate this breeding value given only genomic marker and phenotypic information.

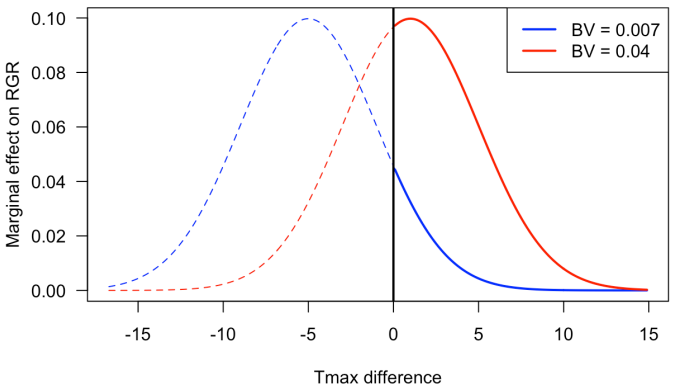

Altogether, we modeled the data-generating process for our simulated progeny growth rates as:

$$Simulated\ RGR = \alpha + Block\_effect + Site\_effect + Family\_effect + Tmax\_difference\_effect + \varepsilon$$

where α is the global intercept set to 1, and residual errors ε are drawn from a normal distribution with mean of 0 and a standard deviation of 0.25. We did not include initial height, locality, or the principal components of the climate of origin in the simulated data generating process to simplify the simulation and modeling process, even though they are included as covariates in the analyses presented in the main text. We do not anticipate the exclusion of these covariates would have an impact on the validity of our simulation results because these components did not have significant interactions with progeny growth rates across T_{max} differences in our empirical dataset.

Statistical Analysis

Using the simulated datasets, we ran the analysis approach presented in the main and supplementary text of this study, which we refer to here as 'SNP-by-SNP GAM analysis', and calculated the Pearson's correlation coefficient between estimated GEBVs from this statistical approach and the 'true' BVs calculated directly from the simulated data. We also wanted to assess alternative statistical approaches, such as a gBLUP (genomic Best Linear Unbiased Predictor) analysis that predicts breeding values based on the genomic relatedness matrix among individuals (36). We ran two separate gBLUP analyses, which differed in how they were estimating and summarizing progeny growth responses when planted into warmer temperatures. First, we used a generalized additive model (GAM) and estimated separate progeny growth response functions across T_{max} differences for each maternal tree by treating the interaction between T_{max} difference and family as a random effect. From these predicted progeny growth responses, we calculated the relative growth rate when planted into warmer temperatures (T_{max} difference > 0°) for each maternal tree and used this maternal tree-level metric as the phenotype for the gBLUP analysis. The benefit of this 'gBLUP-GAM' approach is that the shape of the progeny growth response is flexible and not assumed to take a linear form, though it can be slow to fit models when the sample size is large.

The second gBLUP analysis estimated growth responses across T_{max} differences as a quadratic function in a linear mixed model, such that progeny relative growth rates were a function of T_{max} difference and its squared term, and the 1st order polynomial term was treated as a random effect that varied across maternal trees. This 'gBLUP-Quadratic' approach allows the overall position of the progeny growth response curve to vary for each maternal tree and therefore have different T_{max} difference optimums, though it assumes that the overall curvature of the progeny growth response curve is equivalent across families, which happens to be the case in our

simulated data. We initially tried to have both the 1st and 2nd order polynomial terms vary as random effects across maternal trees, but these models did not converge or produce reliable estimates using this approach with our simulated data sets. As in the gBLUP-GAM, we similarly calculated the relative growth rate of progeny when planted into warmer temperatures for each maternal-tree based on the predicted growth response functions and used this maternal tree-level metric as the phenotype for the gBLUP analysis. The benefit of this gBLUP-Quadratic approach is that it is relatively fast to fit the model, but it assumes a quadratic shape of the progeny growth response function, which may not be accurate in all cases. We fit the growth response models in R v3.5.1 (22) using the 'mgcv' (21) and 'lme4' (45) packages. To conduct the gBLUP analyses, we used two R packages 'BGLR' (46) and 'GAPIT' (47) to estimate the gBLUPs and found the breeding value estimates to be perfectly correlated (R = 1.0) across packages, so we only present results output by BGLR.

Data simulation results

First, we will present an overview of the results from data simulated using 2 planting sites, mirroring the planting design of our empirical dataset and using the approach outlines in the main text (SNP-by-SNP GAMs). Then, we will present results summarizing simulations that varied the number of planting sites, different genetic, architectures, and analysis type (*e.g.*, SNP-by-SNP GAM vs. gBLUP approaches). We found that the overall approach of using GAMs to estimate growth response to T_{max} differences was able to accurately estimate an adaptational lag in temperature at the species level with 2 planting sites, as shown in the figure below with the simulated 'true' species-level growth response shown on the left and the estimated growth response from the GAM analysis on the right. Note that the y-axes are not expected to be equivalent, as the simulated effect is on the left is only the marginal effect on progeny relative growth rates, while the figure on the right incorporates block, site, and accession effects into the overall prediction of progeny relative growth rates.

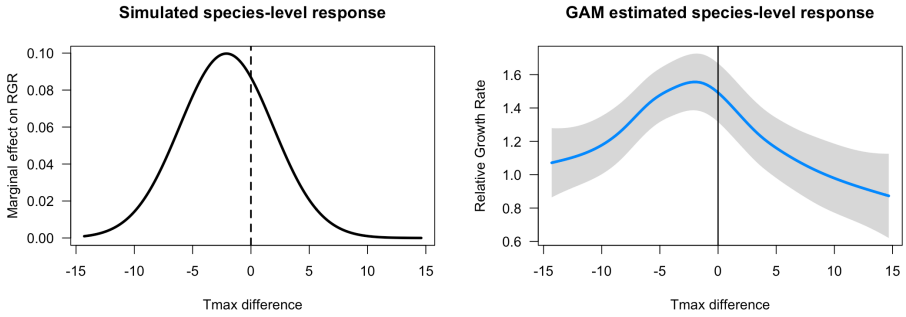

Overall, with simulated data from 2 planting sites, our statistical analysis using GAMs to estimate separate growth responses across T_{max} differences on a SNP-by-SNP basis was able to accurately predict breeding values for progeny growth in warmer temperatures. The figure below shows the correlation between the known true breeding value and the estimated GEBV from the GAM analysis for each simulated genetic architecture. Overall the correlation coefficient was highest when growth response was a polygenic trait (R = 0.63, shown left) and slightly lower when growth response was driven by a few major loci (R = 0.48, shown right).

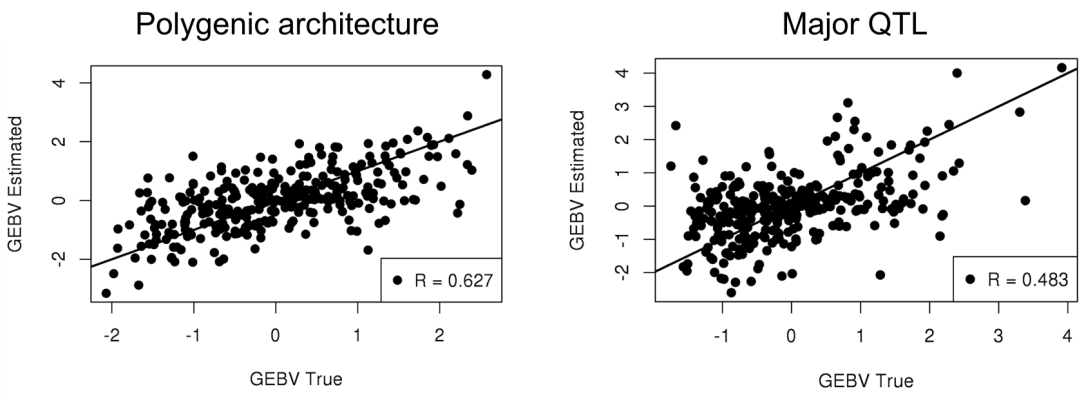

The distribution of estimated uncorrected P-values of the T_{max} difference and SNP interaction from the SNP-by-SNP GAM analysis was somewhat uniformly distributed for the polygenic architecture, and less so for the major QTL architecture. We see similar distributions of P-values with our empirical data with 2 planting sites (Figure S9).

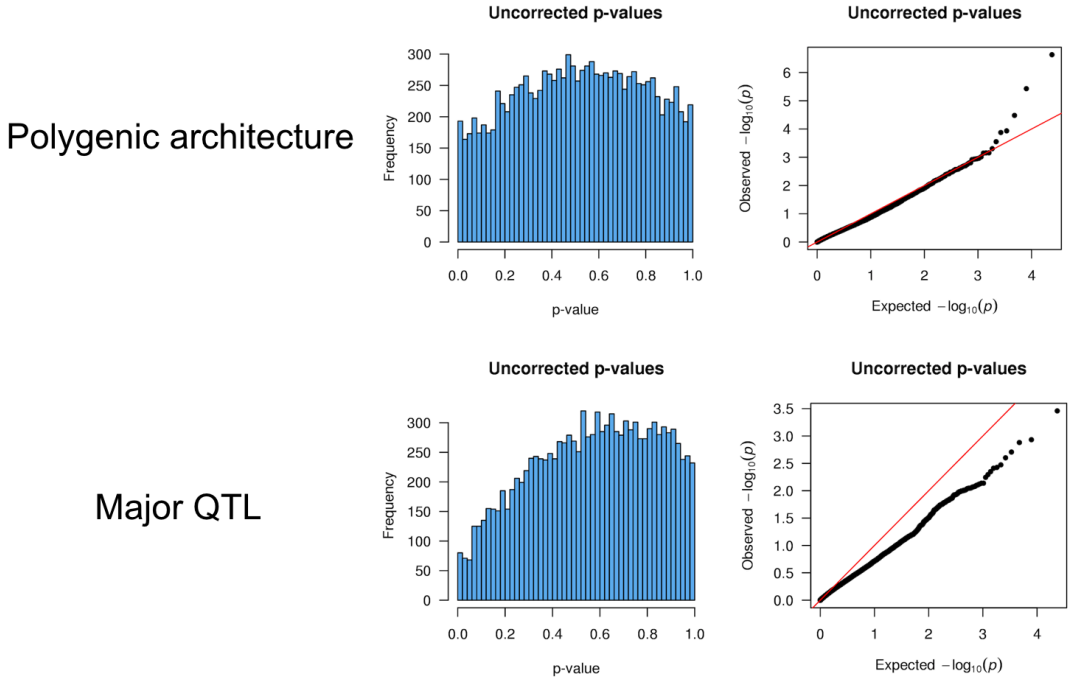

The gBLUP analysis (either using GAMs or quadratic mixed-model regressions) were less effective than the SNP-by-SNP GAM approach at estimating the 'true' breeding values and produced lower correlation coefficients between the true and estimated breeding values. Pearson's R for the gBLUP analyses ranged from 0.13 – 0.24 depending on the method and genetic architecture, shown below.

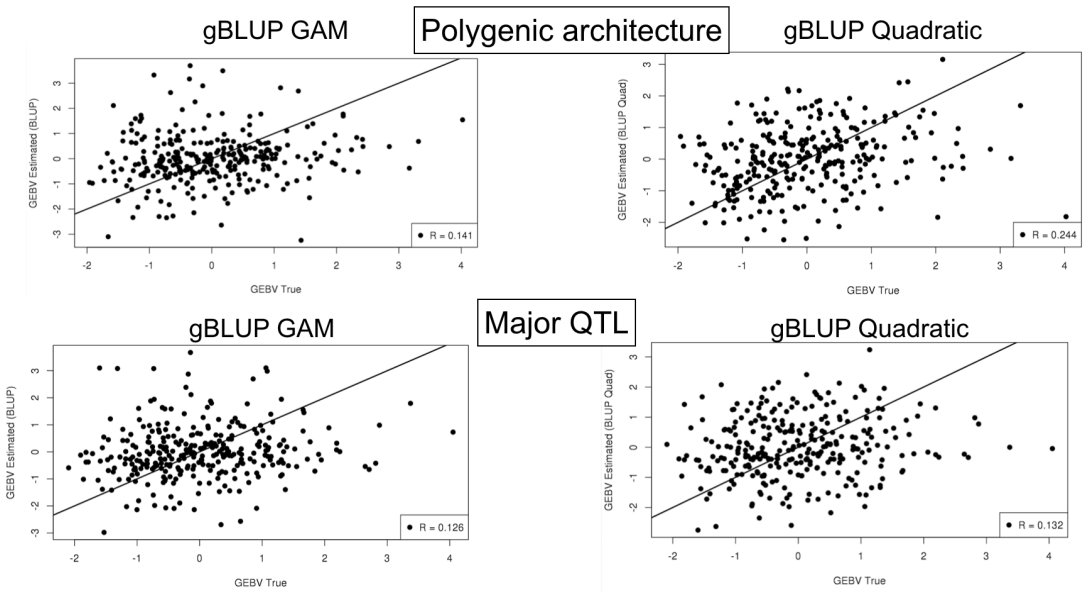

With only 2 planting sites, it is likely that the gBLUP analysis has difficulty estimating the growth response function at the maternal-tree level. Each family in this scenario only has data at 2 values of T_{max} differences, thus making it difficult to estimate the underlying progeny growth response function from just two points along the T_{max} difference axis. To illustrate this, the figure below shows the underlying simulated growth response function for 3 maternal trees, with the corresponding circles showing where the sampling data is coming from at the 2 planting sites on the left (*i.e.*, 2 T_{max} difference values per family). We would expect the efficacy of the gBLUP approach to improve as more planting sites are added to the sampling design, which would allow more complete sampling coverage of the progeny growth response function, as shown on the right panel with 15 simulated planting sites.

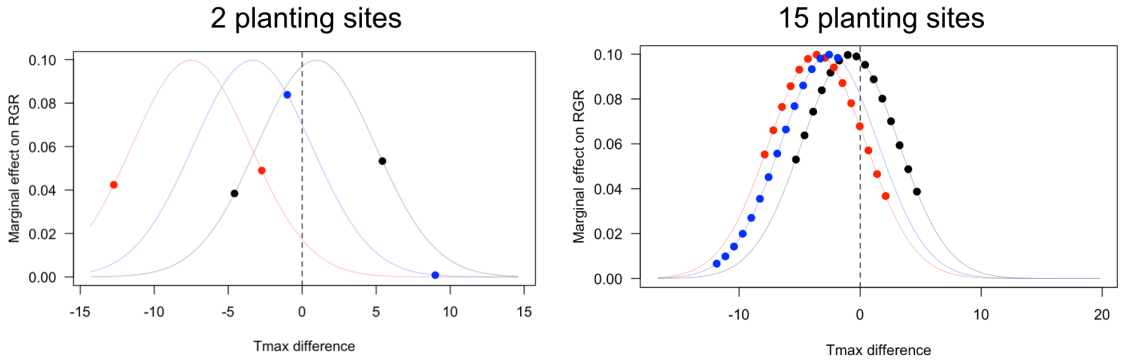

We then simulated datasets ranging with 2, 5, 10, and 20 planting sites and again compared the efficacy of each statistical approach in recovering the true breeding value. We found that, overall, the SNP-by-SNP GAM approach produced higher correlations between the true and estimated breeding values across all simulated number of planting sites. The figure below shows this pattern, with the correlation between the 'true' and estimated breeding values averaged across 10 replicates shown across the range of planting sites, and separated out by modeling approach and genetic architecture:

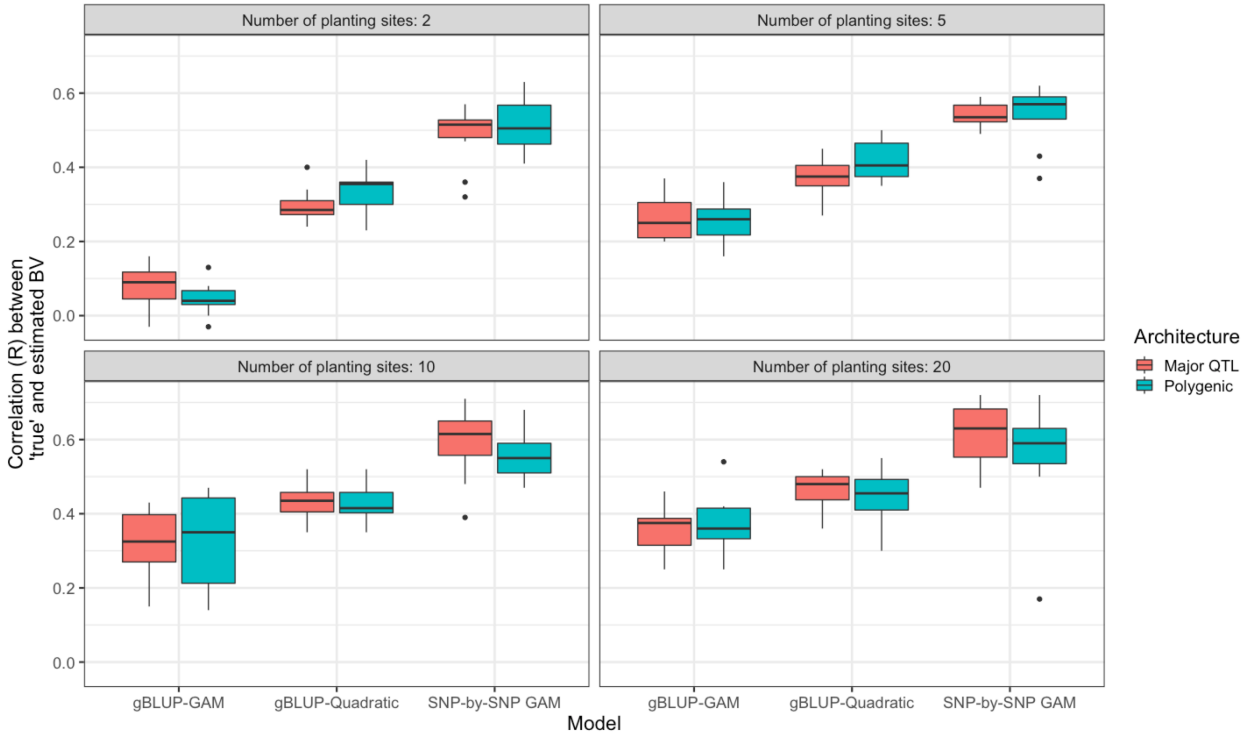

Overall, the data simulation analysis suggests that the SNP-by-SNP GAM approach presented in the main text of this study is more closely aligned with the 'true' underlying breeding values, while being more flexible and robust to smaller sample sizes.

Estimating benefits of genome-informed assisted gene flow

We mapped how GEBVs varied across the valley oak range based on climate and spatial associations. For the 304 genotyped maternal trees with progeny in the provenance trial, we associated their GEBV with their latitude, longitude, latitude x longitude interaction, and elevation of their original location, and a set of climate variables representing their climate of origin that were not strongly correlated: T_{max}, T_{min}, $T_{ave,}$ precipitation seasonality (Bioclim 15), summer precipitation (Bioclim 18), precipitation of the coldest quarter (Bioclim 19), and climatic water deficit (CWD). We used the corresponding climate data from the BCM dataset (5) to generate our map of GEBV predictions. This map (Figure S5) allowed us to then generate predictions of how relative growth rates across the valley oak range would change under a business-as-usual emissions scenario by 2070-2099 (RCP-8.5) based on current GEBV distributions. We then simulated a scenario of genome-informed assisted gene flow where for each potential planting site across the valley oak range (*i.e.*, each cell in the raster encompassing the sample area), we calculated the highest GEBV within a 50 km radius and used this maximized GEBV at each point to estimate how progeny relative growth rates would change if individuals with the highest GEBVs within 50 km of each planting site were used as seed sources.

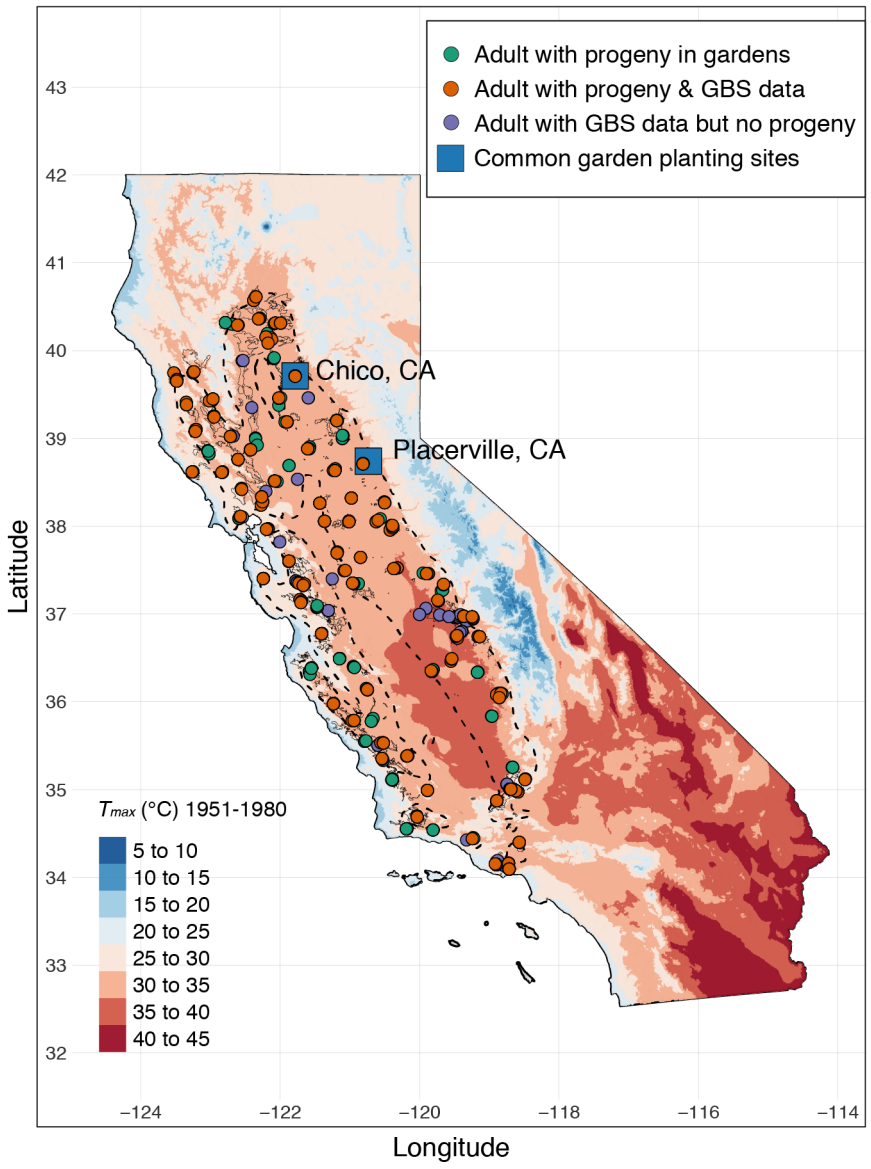

Fig. S1. Map of valley oak samples and T_{max} (°C) 1951-1980 across California. Green circles indicate location of the adults who have progeny in the common garden (n = 659), orange circles indication location of adults who have progeny in the common garden and have genotyping by sequencing (GBS) data (n = 304) which may overlap green circles, and purple circles indicate location of adults who have GBS data but do not have progeny in the common gardens (n = 133). Blue squares show the locations of the common gardens in Chico, CA and Placerville, CA. Dashed black outline shows historical range of valley oak prior to contemporary habitat loss and fragmentation, while lighter grey lines show contemporary populations.

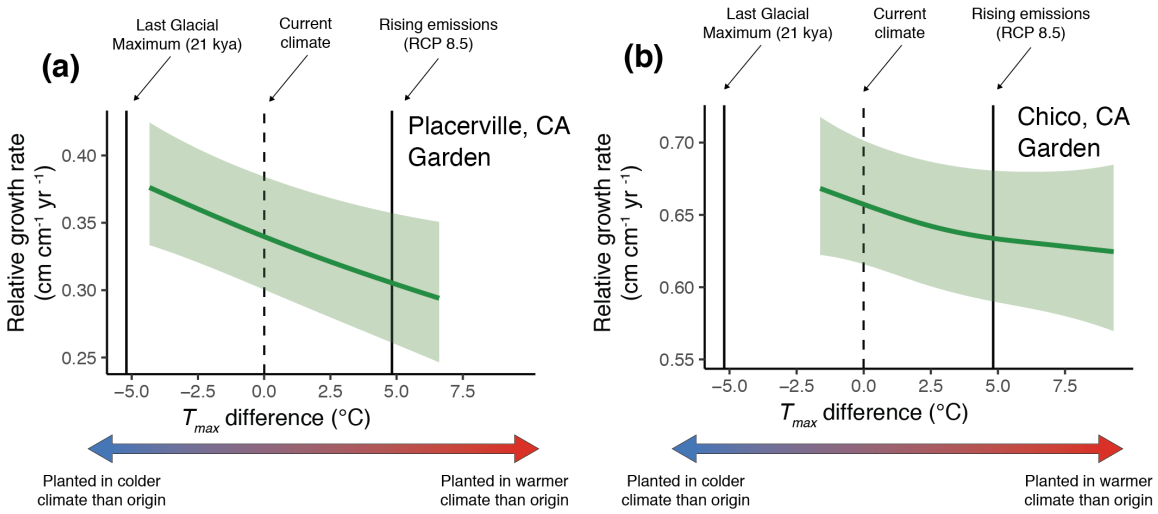

Fig. S2. Predicted relative growth rates and approximate 95% confidence interval for valley oaks across T_{max} difference estimated separately for (a) Placerville, CA and (b) Chico, CA common gardens. Dashed vertical line shows where planting site matches climate of origin (T_{max} difference = 0) and solid lines show T_{max} difference between Last Glacial Maximum 21,000 years ago and current climate (5.2° cooler) and predicted increase in temperature of 4.8° C for rising emissions scenarios by 2100 (RCP 8.5).

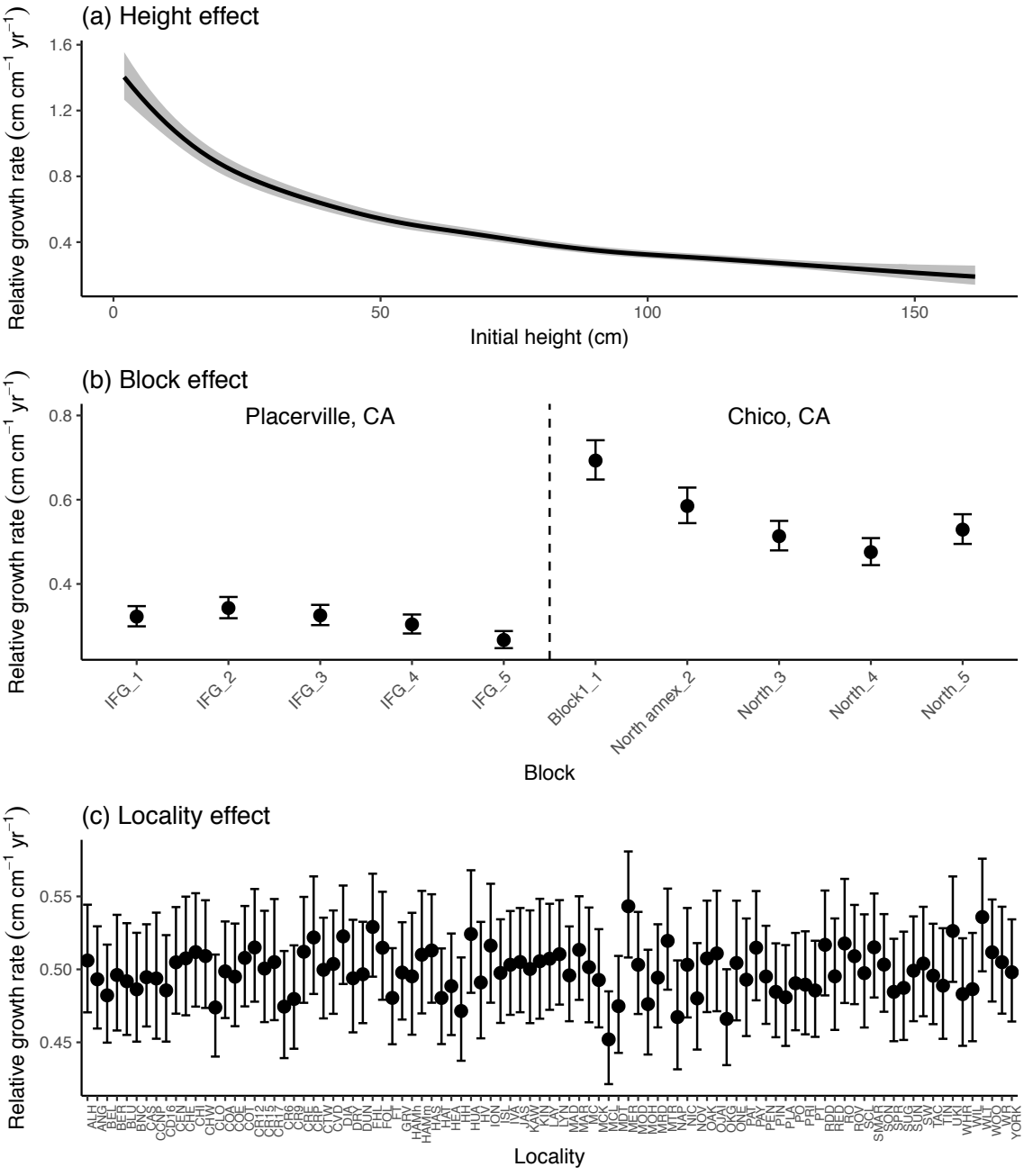

Fig. S3. Predicted relative growth rates and approximate 95% confidence intervals showing: (a) that relative growth rates decline with initial height, (b) that relative growth rates vary across blocks, with higher relative growth rates occurring in Chico, CA common garden compared to Placerville, CA garden, and (c) that relative growth rates vary by locality.

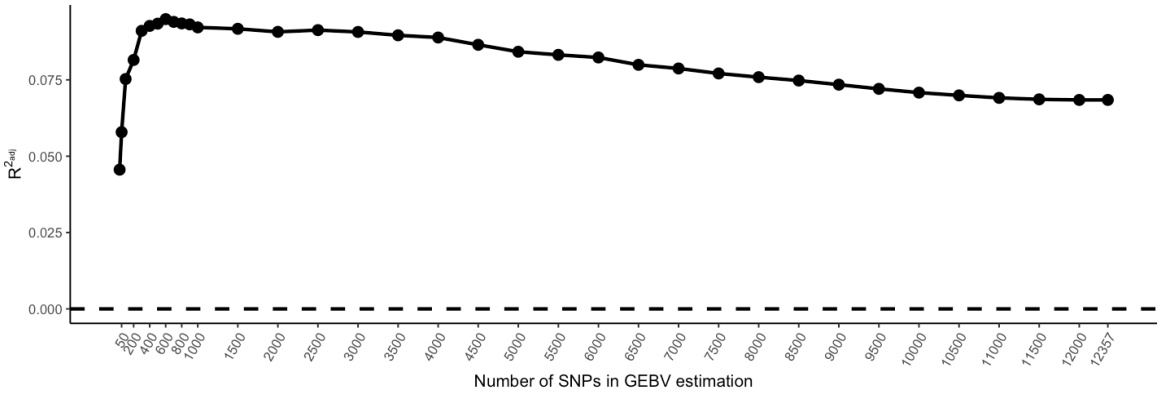

Fig. S4. Variance explained (R^2_{adj}) of adjusted relative growth rates by GEBVs estimated with varying numbers of SNPs in a model of all individuals with maternal genotypes (n = 2,295). Using 600 SNPs with the strongest genotype-by-temperature interactions explained the most amount of variance. Note that the same data is being used to both fit the model and assess its explanatory power. We estimate the predictive power of GEBVs with 10-fold cross-validation in Table S2.

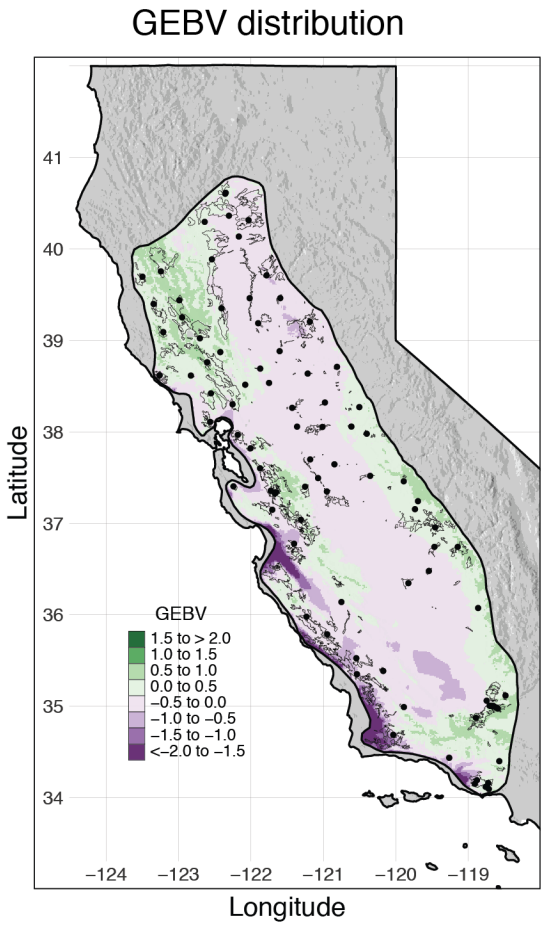

Fig. S5. Landscape distribution of genomic estimated breeding values (GEBVs) for higher growth rates under warmer temperatures based on modeled climate and spatial associations (Table S3). Black circles indicate sampled localities. Light black outlines indicate contemporary valley oak range.

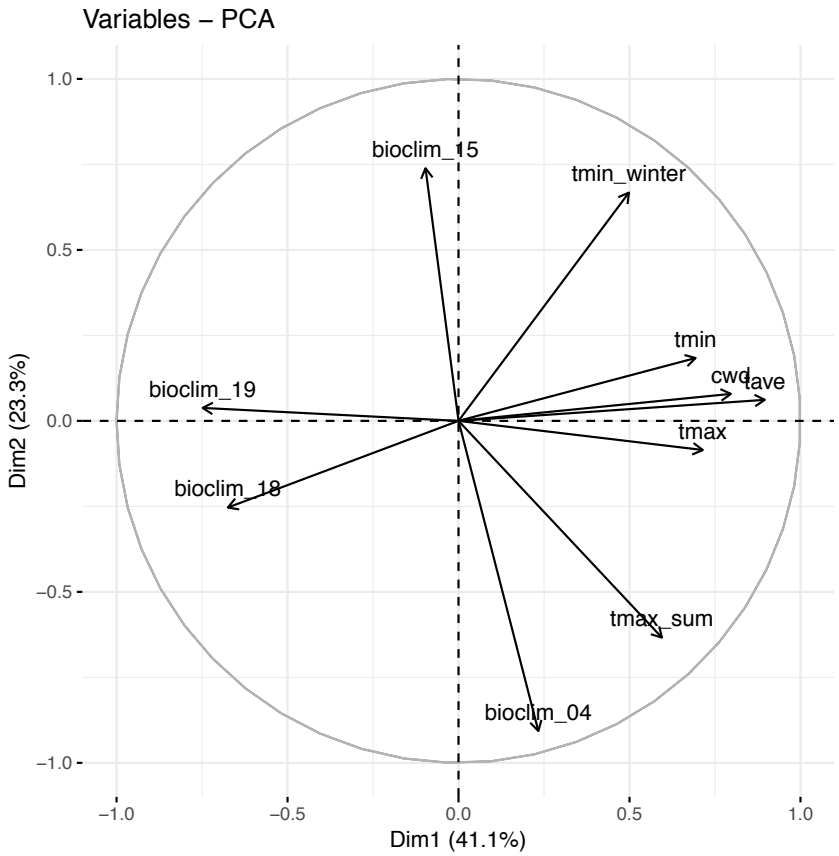

Fig. S6. Biplot of the contributions of climatic variables to the first 2 dimensions of a principal component analysis of the climate of origin for progeny in the valley oak provenance trial. The climate variables we used to characterize climate of origin were maximum summer temperature (T_{max}), average maximum temperature across all months (T_{max_annual}), minimum winter temperature (T_{min}), average minimum temperature across all months (T_{min_annual}), average temperature across all months (Tave), temperature seasonality (Bioclim 4), precipitation seasonality (Bioclim 15), summer precipitation (Bioclim 18), precipitation of the coldest quarter (Bioclim 19), and climatic water deficit (CWD).

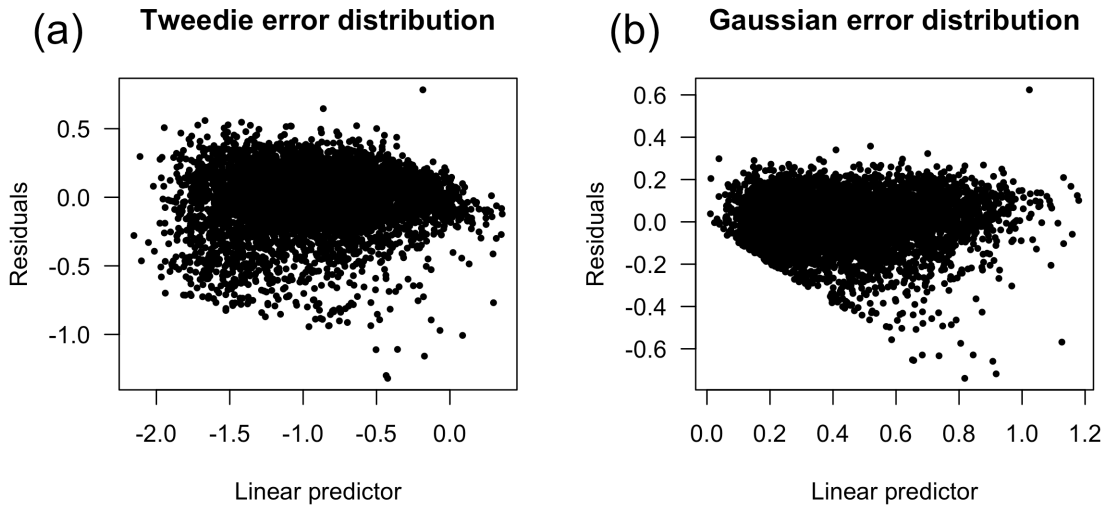

Fig. S7. Linear predictor plotted against residuals from the full model (N = 5,051) individuals) with (a) Tweedie error distribution and (b) Gaussian error distribution. The Tweedie error distribution appears to improve the fit of the model by removing structure in the residuals.

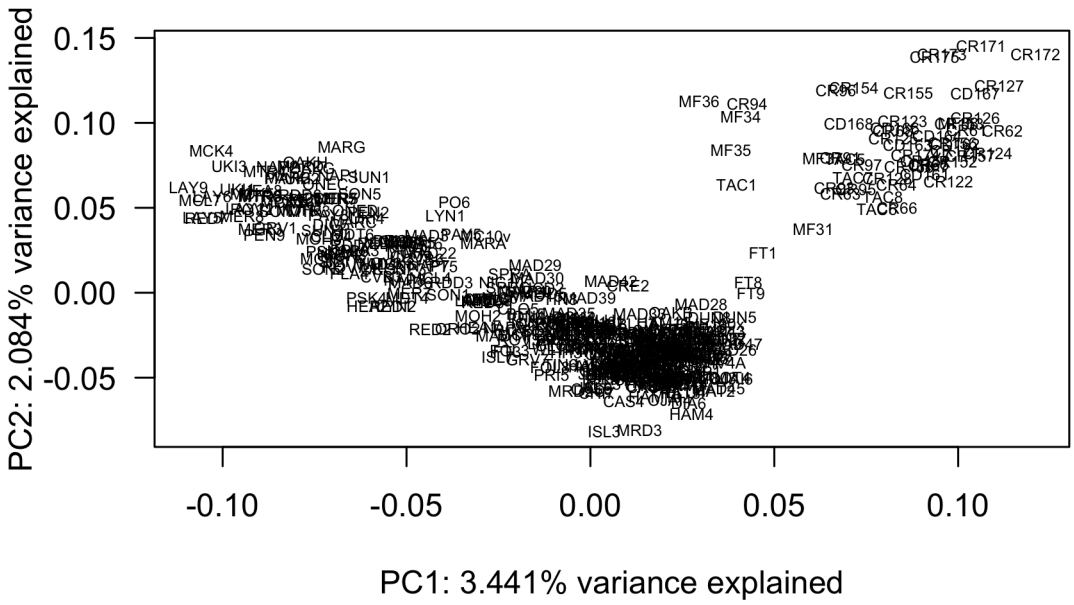

Fig. S8. Biplot of principal components analysis (PCA) on 12,357 SNPs from 421 valley oak adults. Labels indicate the sample ID. The first two PC axes explained 3.4% and 2.1% of the variance, respectively. SNPs were scaled and mean-imputed before calculating the PCA.

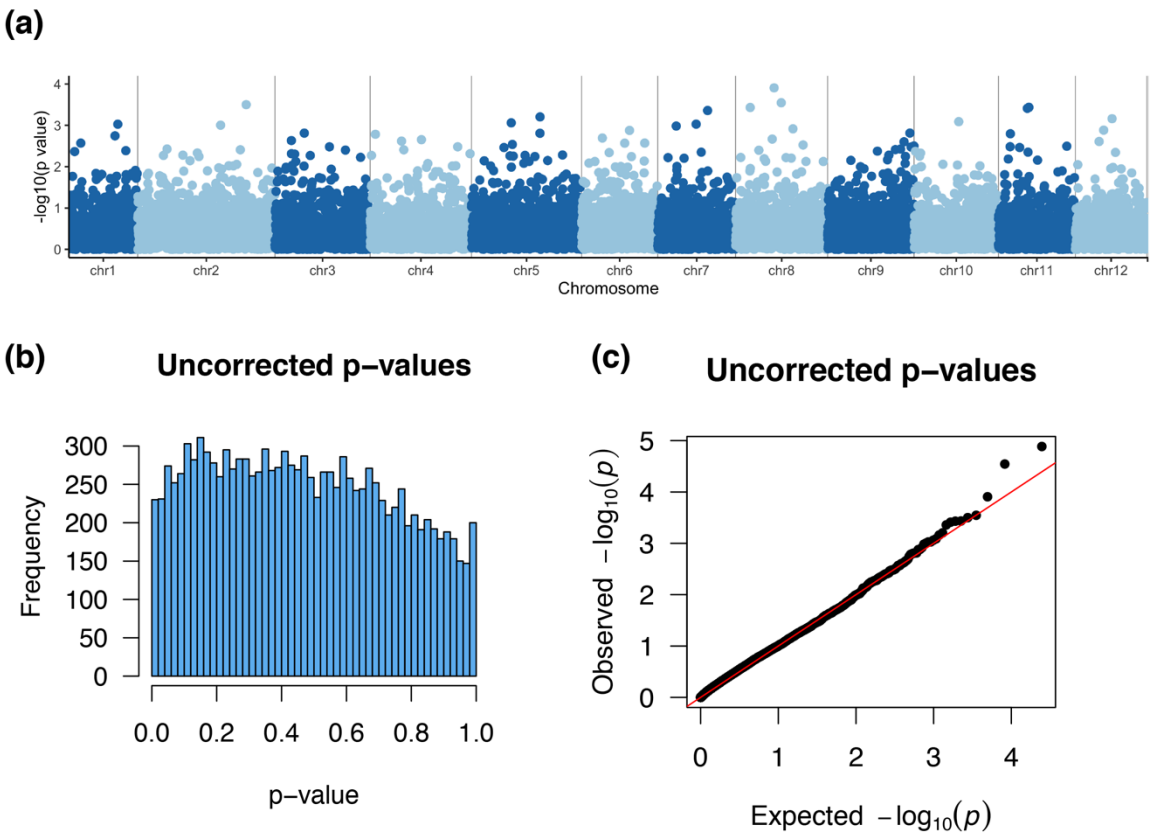

Fig. S9. (a) Manhattan plot showing the strength of genotype by T_{max} difference interactions (uncorrected p value) of 12,357 SNPs across 12 chromosomes of valley oak. **(b)** Histogram and **(c)** QQ-plot of uncorrected p-values from the genome-wide association (GWAS) of the interaction term of genotype with T_{max} difference across 12,357 SNPs based on generalized additive models. Figure 2a in the main text shows the predicted effect size on relative growth rates for each genotype at each SNP represented in the Manhattan plot.

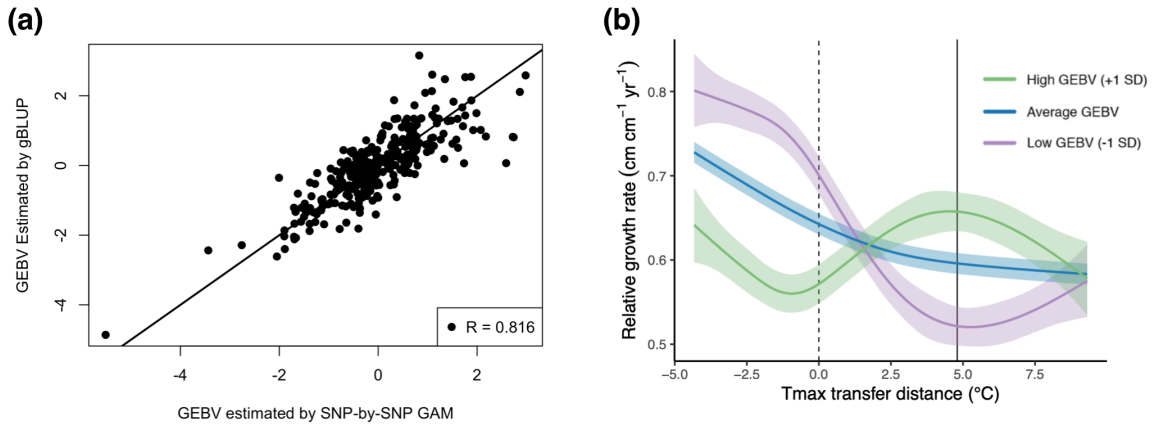

Fig. S10. (a) Correlation between genomic estimated breeding values (GEBVs) estimated by the 'SNP-by-SNP' GAM analysis presented in the main text vs. GEBVs estimated through a gBLUP (genomic Best Linear Unbiased Predictors) analysis. The legend in the bottom right shows the estimated Pearson's correlation coefficient between the two sets of GEBVs (R = 0.816, P < 0.001). **(b)** Contrasting progeny growth responses for T_{max} difference and approximate 95% confidence intervals for maternal trees with genomic-estimated breeding values (GEBV) estimated by the gBLUP analysis for optimal growth rate under warmer temperatures at the average value, +1 SD above average, and -1 SD below average. Dashed vertical line shows where planting site matches climate of origin (T_{max} difference = 0) and solid shows predicted increase in temperature of 4.8° C for rising emissions scenarios by 2100 (RCP 8.5).

Table S1. Parameter estimates from a generalized additive model on relative growth rates (cm cm-1 yr-1) of 5,051 valley oaks planted in two common gardens in California. Estim. df is the estimated degrees of freedom, df is the degrees of freedom, F is the F statistic, and the estimated P value for the smooth terms and parametric coefficients, along with the total variation explained by the full model. Values in bold are parameters where $P < 0.05$.

Parameter	**Estim. df**	**F**	***P* value**
Smooth terms			
T_{max} difference	**2.43**	**5.60**	**0.00076**
$Height_{2014}$	**6.32**	**587.65**	**$< 2e^{-16}$**
Family ID	<0.01	0.00	0.9420
Locality	**44.87**	**0.99**	**$1.56e^{-8}$**
Climate PC1	1.00	0.44	0.510
Climate PC2	<0.01	0.39	0.991
Climate PC1 * T_{max} difference	1.00	0.001	0.982
Climate PC2 * T_{max} difference	5.05	1.23	0.206
Parametric coefficients	**df**		
Block	**9**	**249.6**	**$< 2e^{-16}$**
R^2 adjusted = 0.721			

Table S2. Mean and standard deviation (SD) of the amount of variance explained (R^2_{adj}) in adjusted relative growth rates in independent training sets with 10-fold cross-validation in the observed dataset or in datasets where adjusted relative growth rates were permuted among individuals 100 times. Relative growth rates were adjusted prior to analysis to control for the effects of climate of origin, initial height, locality, family ID, genetic kinship, and the main effect of T_{max} difference (see Methods). The cross-validation approaches either included or did not include individuals from the same family across testing and training sets.

	Observed		**Permuted**	
10-fold cross-validation approach	**R^2_{adj} mean**	**R^2_{adj} SD**	**R^2_{adj} mean**	**R^2_{adj} SD**
No individuals from same family across testing and training sets	0.040	0.033	0.007	0.002
Individuals from same family across testing and training sets	0.035	0.028	0.007	0.001

Table S3. Parameter estimates from a generalized additive model on genomic-estimated breeding values (GEBVs) for 304 genotyped adult valley oaks and spatial and climatic variables. Estim. df is the estimated degrees of freedom, df is the degrees of freedom, F is the F statistic, and the estimated *P* value for the smooth terms, along with the total variation explained by the model. Statistically significant terms (*P* value ≤ 0.05) are shown in bold

Parameter	**Estim. df**	**F**	***P* value**
Smooth terms			
T_{max}	2.34	2.067	0.1161
T_{min}	1.00	1.379	0.2413
Climatic water deficit (CWD)	1.00	1.248	0.2649
Precipitation seasonality (Bioclim_15)	1.00	0.323	0.5702
Summer precipitation (Bioclim_18)	1.00	0.060	0.8071
Elevation	**1.00**	**7.475**	**0.0066**
Latitude	3.28	1.855	0.1078
Longitude	1.00	0.470	0.4934
Latitude x Longitude	**1.409**	**3.345**	**0.0441**
$R^2_{adjusted} = 0.074$			

Supplementary Information References

1. M. K. Anderson (2007) Indigenous uses, management, and restoration of oaks of the far western united states. (United States Department of Agriculture Natural Resources Conservation Service, Washington DC, USA).
2. J. Cavender-Bares, Diversity, distribution, and ecosystem services of the North American oaks. *International Oaks* **27**, 37-48 (2016).
3. B. M. Pavlik, P. C. Muick, S. G. Johnson, M. Popper, *Oaks of California* (Cachuma Press, Los Olivos, CA, 1991).
4. A. Delfino-Mix, J. W. Wright, P. F. Gugger, C. Liang, V. L. Sork (2015) Establishing a range-wide provenance test in valley oak (*Quercus lobata* Née) at two California sites. in *Proceedings of the seventh oak symposium: managing oak woodlands in a dynamic world*, pp 413-424.
5. L. E. Flint, A. L. Flint, J. H. Thorne, R. Boynton, Fine-scale hydrologic modeling for regional landscape applications: the California Basin Characterization Model development and performance. *Ecol. Processes* **2**, 25 (2013).
6. P. F. Gugger, S. J. Cokus, V. L. Sork, Association of transcriptome-wide sequence variation with climate gradients in valley oak (*Quercus lobata*). *Tree Genet. Genomes* **12**, 1-14 (2016).
7. P. F. Gugger, S. Fitz-Gibbon, M. Pellegrini, V. L. Sork, Species-wide patterns of DNA methylation variation in *Quercus lobata* and their association with climate gradients. *Mol. Ecol.* **25**, 1665-1680 (2016).
8. L. M. Kueppers, M. A. Snyder, L. C. Sloan, E. S. Zavaleta, B. Fulfrost, Modeled regional climate change and California endemic oak ranges. *Proc. Natl. Acad. Sci. USA* **102**, 16281-16286 (2005).
9. B. C. McLaughlin, E. S. Zavaleta, Predicting species responses to climate change: Demography and climate microrefugia in California valley oak (*Quercus lobata*). *Global Change Biol.* **18**, 2301-2312 (2012).
10. V. L. Sork *et al.*, Gene movement and genetic association with regional climate gradients in California valley oak (*Quercus lobata* Née) in the face of climate change. *Mol. Ecol.* **19**, 3806-3823 (2010).
11. P. F. Gugger, M. Ikegami, V. L. Sork, Influence of late Quaternary climate change on present patterns of genetic variation in valley oak, *Quercus lobata* Née. *Mol. Ecol.* **22**, 3598-3612 (2013).
12. J. VanDerWal, L. Beaumont, N. Zimmerman, P. Lorch, Climates: methods for working with weather & climate. *R package version 0.1-1.6* (2011).
13. T. Wang, A. Hamann, D. L. Spittlehouse, T. Q. Murdock, ClimateWNA-high-resolution spatial climate data for western North America. *J. Appl. Meteorol. Climatol.* **51**, 16-29 (2012).
14. D. P. van Vuuren *et al.*, The representative concentration pathways: an overview. *Clim. Change* **109**, 5-31 (2011).
15. C. M. Tyler, B. Kuhn, F. W. Davis, Demography and recruitment limitations of three oak species in California. *Q. Rev. Biol.* **81**, 127-152 (2006).

16. R. D. Sage, W. D. Koenig, B. C. McLaughlin, Fitness consequences of seed size in the valley oak *Quercus lobata* Née (Fagaceae). *Annals of Forest Science* **68**, 477 (2011).
17. C. E. T. Paine *et al.*, How to fit nonlinear plant growth models and calculate growth rates: An update for ecologists. *Methods Ecol. Evol.* **3**, 245-256 (2012).
18. B. Jorgensen, Exponential dispersion models (with discussion). *J. Royal Stat. Soc.* **49**, 127-162 (1987).
19. M. C. K. Tweedie (1984) An index which distinguishes between some important exponential families. in *Statistics: Applications and new directions: Proceedings of the Indian Statistical Institute Golden Jubilee International Conference*, pp 579-604.
20. H. Schielzeth, Simple means to improve the interpretability of regression coefficients. *Methods Ecol. Evol.* **1**, 103-113 (2010).
21. S. Wood, Package 'mgcv'. *R package version 1.8-26* **1**, 29 (2015).
22. R. C. Team, R: A language and environment for statistical computing. (2017).
23. R. J. Elshire *et al.*, A robust, simple genotyping-by-sequencing (GBS) approach for high diversity species. *Plos One* **6** (2011).
24. J. M. Catchen, A. Amores, P. Hohenlohe, W. Cresko, J. H. Postlethwait, Stacks: building and genotyping loci de novo from short-read sequences. *G3: Genes, genomes, genetics* **1**, 171-182 (2011).
25. H. Li, R. Durbin, Fast and accurate long-read alignment with Burrows–Wheeler transform. *Bioinformatics* **26**, 589-595 (2010).
26. M. A. DePristo *et al.*, A framework for variation discovery and genotyping using next-generation DNA sequencing data. *Nat. Genet.* **43**, 491 (2011).
27. S. J. O'Leary, J. B. Puritz, S. C. Willis, C. M. Hollenbeck, D. S. Portnoy, These aren't the loci you're looking for: Principles of effective SNP filtering for molecular ecologists. *Mol. Ecol.* **27**, 3193-3206 (2018).
28. P. Danecek *et al.*, The variant call format and VCFtools. *Bioinformatics* **27**, 2156-2158 (2011).
29. S. Purcell *et al.*, PLINK: a tool set for whole-genome association and population-based linkage analyses. *Am. J. Hum. Genet.* **81**, 559-575 (2007).
30. M. G. Naylor, S. T. Weiss, C. Lange, Recommendations for using standardised phenotypes in genetic association studies. *Hum. Genomics* **3**, 308-319 (2009).
31. D. J. Balding, A tutorial on statistical methods for population association studies. *Nat. Rev. Genet.* **7**, 781-791 (2006).
32. A. Korte, A. Farlow, The advantages and limitations of trait analysis with GWAS: a review. *Plant Methods* **9**, 29 (2013).
33. J. B. Endelman, Ridge regression and other kernels for genomic selection with R package rrBLUP. *Plant Genome* **4**, 250 (2011).
34. K. M. Hernandez, Understanding the genetic architecture of complex traits using the function-valued approach. *New Phytol.* **208**, 1-3 (2015).
35. J. R. Stinchcombe, G. Function-valued Traits Working, M. Kirkpatrick, Genetics and evolution of function-valued traits: understanding environmentally responsive phenotypes. *Trends Ecol. Evol.* **27**, 637-647 (2012).
36. P. Gienapp *et al.*, Genomic quantitative genetics to study evolution in the wild. *Trends Ecol. Evol.* **32**, 897-908 (2017).

37. Z. A. Desta, R. Ortiz, Genomic selection: genome-wide prediction in plant improvement. *Trends Plant Sci.* **19**, 592-601 (2014).
38. T. H. Meuwissen, B. J. Hayes, M. E. Goddard, Prediction of total genetic value using genome-wide dense marker maps. *Genetics* **157**, 1819-1829 (2001).
39. J. Crossa *et al.*, Genomic selection in plant breeding: Methods, models, and perspectives. *Trends in Plant Sciences* **22**, 961-975 (2017).
40. D. Grattapaglia, M. D. V. Resende, Genomic selection in forest tree breeding. *Tree Genet. Genomes* **7**, 241-255 (2011).
41. J. R. Lasky *et al.*, Genome-environment associations in sorghum landraces predict adaptive traits. *Sci. Adv.* **1**, e1400218 (2015).
42. N. R. Wray *et al.*, Pitfalls of predicting complex traits from SNPs. *Nat. Rev. Genet.* **14**, 507-515 (2013).
43. D. S. Falconer, T. F. C. Mackay, *Introduction to quantitative genetics* (Longmans Green, Harlow, Essex, UK, 1996).
44. D. Grivet, J. J. Robledo-Arnuncio, P. E. Smouse, V. L. Sork, Relative contribution of contemporary pollen and seed dispersal to the effective parental size of seedling population of California valley oak (Quercus lobata, Née). *Mol. Ecol.* **18**, 3967-3979 (2009).
45. D. Bates, M. Maechler, B. Bolker, S. Walker, Fitting linear mixed-effects models using lme4. *J. Stat. Softw.* **67**, 1-48 (2015).
46. P. Perez, G. de los Campos, Genome-wide regression and prediction with the BGLR statistical package. *Genetics* **198**, 483-495 (2014).
47. Y. Tang *et al.*, GAPIT Version 2: an enhanced integrated tool for genomic association and prediction. *Plant Genome* **9** (2016).